5th International Conference on Experimental Fluid Mechanics ICEFM 2018 Munich
Munich, Germany, July 2-4, 2018

Experimental investigation of flow pulsation waveforms in rectangular mesochannels for high heat flux electronics cooling

Jaakko McEvoy[1*], Sajad Alimohammadi[1], Tim Persoons[1]

[1] Trinity College Dublin, Department of Mechanical & Manufacturing Engineering, Dublin, Ireland

[*] jmcevoy@tcd.ie

Abstract

The ever rising heat fluxes encountered in electronic devices present a challenging thermal engineering problem, and one which often requires further miniaturization of the cooling element which should mitigate this heat load and ensure a limited device operating temperature. The scope of this work only extends to heatsinks with internal single phase liquid flows, due to the added complexity of visualization and stable operation of two phase-flows at the microscale. With the rapid advancement in microfabrication techniques, the research community has been locked in a race to study the smallest possible structures with an aim of improved heat transfer. While the added cooling ability of two phase flows and small hydraulic diameter microchannels is attractive, there now exists a large gap in the knowledge between micro and macrochannel structures. This work aims to fill a part of that gap with an analysis of the fluid dynamics of mesochannels ($d_h = 770 \mu m$) under steady and pulsating flows. The effects of pulsation have been shown to increase heat transfer under certain conditions, while the majority of previous research has focused on only sinusoidally oscillating flows, this work investigates the effect of a sinusoidal, triangular and asymmetric sine wave on flow pulsation for Womersley numbers = 1.0, 2.2, 4.1 and 5.0.

1 Introduction

Traditionally low heat flux devices could be cooled by forced convection of cooled air, but with the rapid advances in microprocessor technology there exists a growing need to effectively cool heat fluxes as high as 300 W/cm^2, with the number predicted to rise to over 1000 W/cm^2 in the near future. The first example of the feasibility of using microchannels to combat high heat fluxes was demonstrated in the pioneering work of Tuckerman and Pease (1981).They demonstrated the ability to remove heat fluxes of 790 W/cm^2 in integrated silicon circuits. Their work inspired others to consider microchannel technologies for high heat flux removal from small scale applications to large industrial and aerospace applications. Oscillating fluid interfaces have been shown to enhance heat transfer under certain circumstances and have been of interest since Stokes' second problem in 1851, where a one-dimensional flat plate oscillating in the streamwise direction was considered by Stokes (1851). The problem solves for the transverse velocity oscillations from the plate, which decay with increased distance from the plate. The oscillation from the plate propagates as a dampened wave normal to the direction of oscillation, with the oscillating amplitude reducing to 1% at a distance known as the Stokes boundary layer thickness δ. The oscillating conditions within a channel can be described by the non-dimensional Womersley number, which represents the ratio of transient to viscous forces as introduced by Womersley (1955). Flow pulsation and oscillation in single phase fluids with an aim for improved heat transfer from macro scale to the nano scale has been studied before using a range of different methodologies. Denison and Stevenson (1970) used a directionally sensitive laser velocimetry methodology to measure unsteady oscillating flows for $1.71 \leq \text{Wo} \leq 14.1$. Clamen and Minton (2006) studied the effect of an oscillating pipe on the contained flow for a Reynolds number range of 1275 - 2900, and found good agreement with laminar theory at the low end of the range, but some deviation at higher *Re*. Ojha et al. (1988) demonstrated the effectiveness of a photochromatic dye excited by a laser to capture a snapshot of the fluid flow profile, with good agreement to Womersley's model flow. Blythman et al. (2017) used experimental PIV data to verify their analytical model for a two dimensional rectangular channel, with good agreement. Ray et al. (2005) were one of the few who have studied non-sinusoidal driven excitation waveforms. They used a hot-wire probe and multiple pressure sensors to validate their analytical model for a wide range of *Wo* = 0.15 - 21 and a sinusoidal and triangular waveform. Roslan et al. (2016) conducted a purely analytical study on the effect of waveform on heat transfer for laminar duct flows. They concluded that the excitation waveform does play a notable role in heat transfer performance. Mehta and Khandekar (2015) studied pulsation in square channel using infra-red thermography to analyze the effect of heat transfer for Womersley numbers of 0.8, 3.4, 5.9. They concluded that for $Wo < 0.8$ pulsation has a negative effect on heat transfer, as the diffusion time scale is similar to the time scale of excitation. For higher frequencies (*Wo* = 3.4 and 5.9), the convection term dominates, resulting in small enhancement, but not of any use in real life cooling applications. On the other hand, research by Persoons et al. (2012) indicates the effect of high amplitude pulsation may be able to improve heat transfer in minichannels by up to 40% at low to moderate Reynolds numbers. This paper aims to offer an introduction into the effect of waveform shape and frequency on phased locked velocity profiles and associated pressure drop in pulsatile flow in mesochannel heatsinks, under conditions representative of high heat flux electronics cooling.

2 Experimental approach

The test section consists of an array of 21 rectangular channels with widths of 0.58 *mm* and heights of 1.15 *mm*. Each channel is 25 *mm* long and micro-milled into a copper block. The copper block sits within a PEEK housing and is covered with a 1.15 *mm* thick glass slide to allow full optical access to all channels. The entire assembly is tightly clamped with an aluminium cover cap, with 16 individual tightening screws along the perimeter. A Bronkhorst M15 mass flow meter is used for high accuracy flow measurements. Two differential pressure transducers are used to measure the pressure drop, one across the entire test section (Omega 0-35 *kPa* custom pressure transducer) and the other across the central channel (Honeywell 26PC pressure transducer 0-1 *psi*), through 0.2 *mm* pressure tap holes. The fluid is driven by a Fluidotech FG200 series magnetic drive gear pump, which offers smooth pulseless flow. For accurate monitoring of microscope stage location two Omron ZX-L-N laser displacement sensors are used in the X and Y directions. Flow pulsation is achieved through a Noliac piezo ring bender (CMBR08) driven by two high voltage power supplies and housed in a custom-built chamber located directly before the test section. One power supply (EA-PS 8360-10T) is used to supply a 0-200V constant voltage across the piezo element, with the second power supply (Trek model 2205) being used to amplify the control voltage from 0-4V to 0-200V. The waveforms seen in Fig.1 are generated by a TTi TG315 function generator and monitored on an IDS-1054B oscilloscope and through LabView. The implicit recursive function shown in Eq.(1) describe the leading and lagging waveforms. Where a determines the amplitude, f the frequency, t the time step, k controls the skewness of the function, ($-1 \leq k \leq 1$ = leading to lagging waveform). The leading function waveform, shown in Fig.1(c) will be referred to as $F_{(-1)}$, and the lagging function in Fig.1(d) as $F_{(1)}$, with both $F_{(-1)}$ and $F_{(1)} = y^{(N)}$, with $y^{(N)}$ defined in Eq.(1).

$$For \quad n = 1 \; to \; N; \qquad y^{(n+1)} = a.(sin(2\pi.f.t - k.y^{(n)}/a) - sign(k).y^{(n)}) \tag{1}$$

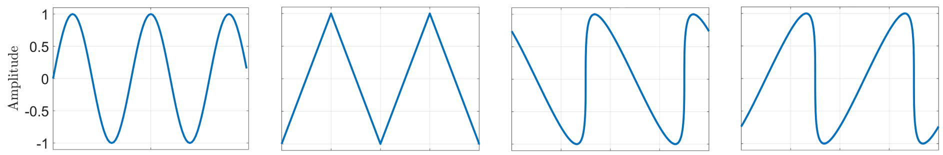

(a) Sine (b) Triangle (c) Leading ($F_{(-1)}$) (d) Lagging ($F_{(1)}$)

Figure 1: Excitation waveforms.

A SM-LVDT displacement transducer mounted along the control rod for the oscillating diaphragm is used to monitor the oscillating signal, to ensure the full stroke length is completed even at high frequencies. A TTL signal generated by the TG315 is used to trigger the image capture when a rising edge is detected in the waveform. This allows for all recordings to begin at the same phase for each waveform considered. The in-house built μ-PIV setup is built around a Zeiss Axio.Vert A1 epifluorescent microscope with a Nikon $10 \times /.40$ objective. Seeding used is Nile Red doped $1.1\mu m$ polystyrene particles from Spherotech. A 1024×1024 pixel Photron SA1.1 high-speed camera is used for image capture, through LaVision DaVis 7.2. To ensure the seeding was as monodisperse as possible, the suspension was sonicated for 15 minutes before tests to give $\sim 90\%$ singles. With μ-PIV, there are often issues related to low seeding density and poor signal to noise ratio, especially with low numerical aperture objectives, such as the one used in this work. A similar image pre-processing methods to the one outlined by Lindken et al. (2006) for their self-calibration procedure is used to reduce the adverse effect of stuck seeding along the channel walls. A sliding maximum was used to increase the seeding density to acceptable levels as outlined by Raffel et al. (2007).

3 Results and Discussion

The effect of oscillation using sinusoidal and non-sinusoidal waveforms on velocity and pressure drops are reported for a mean Reynolds number of 149, and Womersley numbers of 1.0, 2.2, 4.1 and 5.0 (f = 1.00, 5.00, 16.55 and 25.00Hz). A steady (0Hz) case was also tested and compared to the analytical solution for validation of the method. All μ-PIV measurements were taken in a region of fully developed flow in the central channel far downstream of the entrance. The flow velocity experienced is very high due to the small cross-sectional area. This results in the effect of the near wall oscillation being enveloped in the flow. The piezo actuator was used to control the flow oscillation with minimal oscillation amplitudes Q_t/Q_0, in the region of 0.0542, where Q_t is the oscillating flow rate amplitude and Q_0 is the steady flow rate. The effect of these parameters can be most clearly be seen at low frequencies (1Hz), where the oscillating velocity is approximately 5% of the mean velocity for a sinusoidal and triangular waveform. Analysis of the LVDT displacement sensor showed that the triangular wave was only slightly distorted at the highest frequency (25 Hz), but still reached 96% of the full stroke amplitude at lower frequencies. The waveform amplitude was not affected at any other frequency. The primary low order behaviour of the triangular wave is therefore very similar to the sine wave, and the behaviour of the system was not found to be very sensitive to the higher order harmonics of the triangle wave, as discussed below. It was noted that at higher frequencies the asymmetric functions exhibited a lag in time along their vertical impulse stroke.

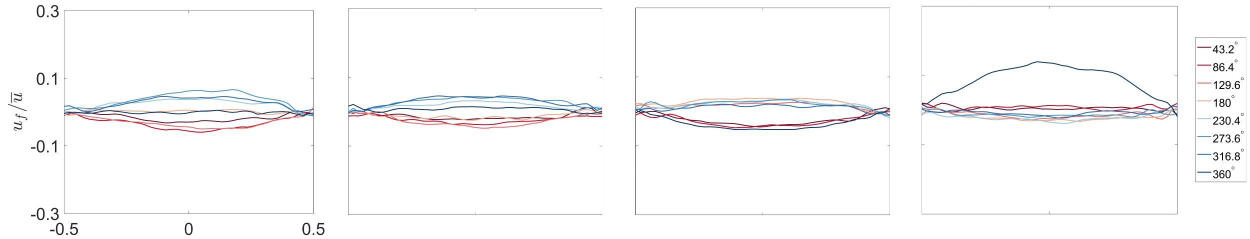

(a) Sine (b) Triangle (c) $F_{(-1)}$ (d) $F_{(1)}$

Figure 2: Phase-averaged fluctuating velocity profiles at f= 1.00Hz ($Wo = 1.0$).

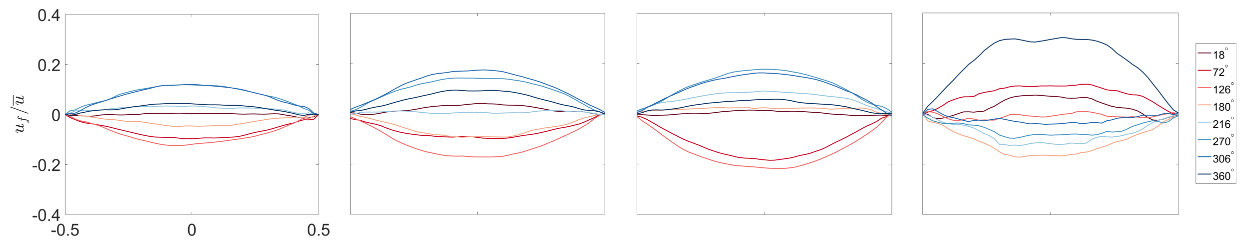

(a) Sine (b) Triangle (c) $F_{(-1)}$ (d) $F_{(1)}$

Figure 3: Phase-averaged fluctuating velocity profiles at f= 5.00Hz ($Wo = 2.2$).

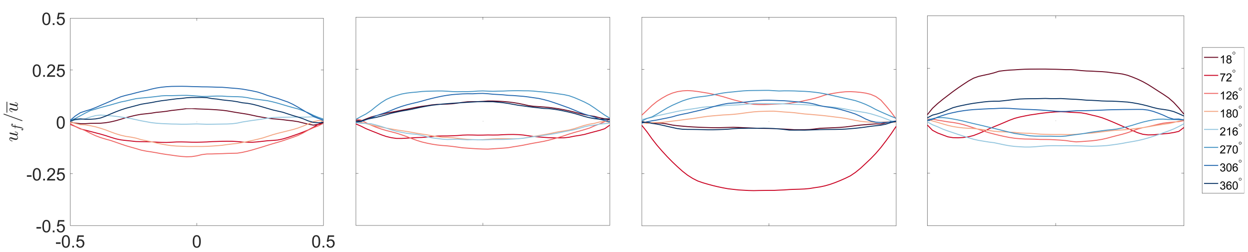

(a) Sine (b) Triangle (c) $F_{(-1)}$ (d) $F_{(1)}$

Figure 4: Phase-averaged fluctuating velocity profiles at f= 16.55Hz ($Wo = 4.1$).

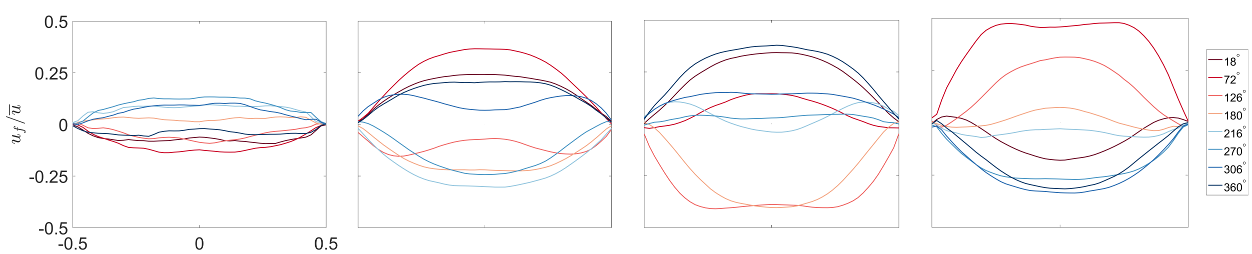

(a) Sine (b) Triangle (c) $F_{(-1)}$ (d) $F_{(1)}$

Figure 5: Phase-averaged fluctuating velocity profiles at f=25.00Hz ($Wo = 5.0$).

The effect of the asymmetric waveforms ($F_{(-1)}$ and $F_{(1)}$) on the fluctuating velocity is immediately clear from Fig.2(d) above. Due to the relatively low velocity fluctuation at low frequencies in the flow, the phase-averaged fluctuating velocity profiles exhibit significant variation across the span of the channel. The fluctuating components of velocity are calculated by subtracting the mean profile of all instances. The sharp up/down-stroke in both asymmetric functions ($F_{(-1)}$ and $F_{(1)}$) oscillations causes a rapid shift in the flow velocity, where inertial forces prevail for a brief period. At the wall the viscous stresses retard the fluid momentum and switch rapidly with varying pressure gradients, resulting in the over/undershoots visible in Fig.2(c) & (d). As the excitation frequency is increased, the effect of the rapidly accelerating and decelerating flow can clearly be seen in either the triangular waveform and both asymmetric function waveforms, due to their sharp inflection points. The leading function ($F_{(-1)}$) described by Eq. (1), exhibits lower fluctuating amplitudes compared to the right skewed ($F_{(1)}$) function. This is due to the direction of the steep impulse stroke imposed upon the flow. For $F_{(-1)}$, the imposed rapid acceleration is in the direction of flow resulting in very low velocity fluctuation over one cycle, but increasing the overall pressure drop in the channel averaged over one cycle due to the momentary increased mean flow velocity. Analysis of the associated wall shear stress and pressure drop was also recorded and will be discussed in greater detail in a following study. For $F_{(1)}$ the direction of the impulse is opposite to the overall flow, resulting in momentary high fluctuations and reduced overall pressure drop. The pressure gradient, dp/dx calculated from the μ-PIV velocity fields rise with increased fluctuations as expected. At f=5Hz the now rapidly switching pressure gradients within the viscous dominated near-wall region leads to the flow profiles displaying the annual effect. Further increasing the frequency to 16.55Hz and 25Hz, the flow begins to loose its quasi-steady characteristics. At 25Hz both asymmetric functions demonstrate approximately similar amplitudes of velocity fluctuation indicating that the waveform acts more as a pure impulse function, and would have little to no variation at higher frequencies. Although not shown here at higher frequencies, it was noted that pressure readings from the more sensitive 26PC pressure transducer exhibited a higher order oscillation for non-sinusoidal waveforms, with a frequency around 50Hz. This was found to be the Helmholtz resonant frequency which was excited by the sharp impulse-like waveforms. Considering the stiffness of the tubing and test section along with the associated fluid, the combined system Helmholtz resonance frequency was estimated to be $45 \leq 55Hz$ for the system. The effect of sinusoidal oscillation on heat transfer has provided inconclusive results in the past, with many studies finding negligible or adverse effects. Most of these studies used a pure sinusoidal waveform, which has been shown here to have a low impact on the mean flow oscillating amplitude and therefore may explain its inefficient narrowing of the thermal boundary layer. The scaling of the velocity fluctuation with increasing frequency is also significantly lower for the pure sinusoidal tests. While higher amplitudes of fluctuation are found with the $F_{(1)}$ waveform, this is due to rapid deceleration and possible flow reversal at lower flow rates, which may have a negative effect on heat transfer as warmer fluid is pulled back towards the entrance of the channel, reducing the overall temperature difference across the heat sink.

4 Conclusion

The effects of varying waveform and frequency on single phase fully developed flow within a mesochannel heat sink array has been demonstrated, though an experimental μ-PIV approach. The effect of pure sinusoidal oscillation was shown to have the least predicted impact on possible heat transfer enhancement, as is suggested in the literature. For a Womersley number range of Wo = 1 - 5, the sinusoidal waveform effects showed negligible alteration. Similar results are observed for a triangular waveform, with the exception of high frequency where the system acts more like an impulse-driven oscillation. The two asymmetric functions display some interesting preliminary results for transient velocity fluctuations, without a large pressure drop trade-off. Further research is required in the area of heat transfer and entrance/exit locations. Future studies should focus on discretizing the near wall region of the channel under higher magnification. The analytical investigation of the asymmetric waveforms should be investigated for comparison with experimental data.

Acknowledgements

This work has emanated from research conducted with the financial support of Science Foundation Ireland under the SFI Strategic Partnership Programme Grant Number SFI/15/SPP/E3125. The authors also would also like to acknowledge the support of the Irish Research Council (IRC) under grant number GOIPD/2016/216.

References

Blythman R, Persoons T, Jeffers N, Nolan KP, and Murray DB (2017) Localised dynamics of laminar pulsatile flow in a rectangular channel. *International Journal of Heat and Fluid Flow* 66:8–17

Clamen M and Minton P (2006) An experimental investigation of flow in an oscillating pipe. *Journal of Fluid Mechanics* 81:421–431

Denison EB and Stevenson WH (1970) Oscillatory Flow Measurements with a Directionally Sensitive Laser Velocimeter. *Review of Scientific Instruments* 41:1475–1478

Lindken R, Westerweel J, and Wieneke B (2006) Stereoscopic micro particle image velocimetry. *Experiments in Fluids* 41:161–171

Mehta B and Khandekar S (2015) Local experimental heat transfer of single-phase pulsating laminar flow in a square mini-channel. *International Journal of Thermal Sciences* 91:157–166

Ojha M, Hummel RL, Cobbold SC, and Johnston KW (1988) Development and evaluation of a high resolution photochromic dye method for pulsatile flow studies. *Journal of Physics E: Scientific Instruments* 21:998

Persoons T, Saenen T, Van Oevelen T, and Baelmans M (2012) Effect of Flow Pulsation on the Heat Transfer Performance of a Minichannel Heat Sink. *Journal of Heat Transfer* 134:091702 (7 pp.)

Raffel M, Willert C, Wereley S, and Kompenhans J (2007) *Particle Image Velocimetry, A Practical Guide*. Springer. second edition

Ray S, Ünsal B, Durst F, Ertunc Ö, and Bayoumi OA (2005) Mass Flow Rate Controlled Fully Developed Laminar Pulsating Pipe Flows. *Journal of Fluids Engineering* 127:405–418

Roslan R, Abdulhameed M, Hashim I, and Chamkha AJ (2016) Non-sinusoidal waveform effects on heat transfer performance in pulsating pipe flow. *Alexandria Engineering Journal* 55:3309–3319

Stokes GG (1851) On the effect of the internal friction of fluids on the motion of pendulums. *Transactions of the Cambridge Philosophical Society* 9:8

Tuckerman DB and Pease RFW (1981) High-performance heat sinking for VLSI. *IEEE Electron Device Letters* 2:126–129

Womersley JR (1955) Method for the calculation of velocity, rate of flow and viscous drag in arteries when the pressure gradient is known. *The Journal of Physiology* 127:553–563